# Controlling spectral selectivity in optoelectronics via photonic band engineering in absorbing media

Botong Qiu
Electrical and Computer
Engieering
Johns Hopkins University
Baltimore, USA
bqiu4@jhu.edu

Yida Lin
Electrical and Computer
Engineering
Johns Hopkins University
Baltimore, USA
ylin89@jhu.edu

Lulin Li
Electrical and Computer
Engineering
Johns Hopkins University
Baltimore, USA
Ili78@jhu.edu

Ebuka S. Arinze
Electrical and Computer
Engineering
Johns Hopkins University
Baltimore, USA
ebuka.arinze@jhu.edu

Susanna M. Thon
Electrical and Computer
Engineering
Johns Hopkins University
Baltimore, USA
susanna.thon@jhu.edu

Arlene Chiu
Electrical and Computer
Engineering
Johns Hopkins University
Baltimore, USA
achiu6@jhu.edu

Abstract— The most common solution for achieving arbitrary spectral selectivity in optoelectronic devices is adding external filters. Here we propose using semiconductor thin film photonic crystals with relevant photonic bands that fall within the absorbing frequency range of the material for spectral selectivity. Optical simulations show that the in-plane photonic bands couple strongly to normal-incidence external fields, inducing tunable resonance features in the out-of-plane transmission and reflection spectra. Experimentally, we fabricate proof-of-principle photonic structure with enhanced visible transparency, consisting of a self-assembled polystyrene bead array infiltrated with colloidal quantum dots, showing promise for multijunction and transparent photovoltaics.

 $\begin{tabular}{lll} Keywords-Photonic & Crystals, & Optoelectronics, & Spectral \\ selectivity & \end{tabular}$ 

# I. INTRODUCTION

Spectrally selective response is of great signicance for many optoelectronic technologies such as finite-bandwidth sensing, detection[1]–[4] and solar energy harvesting [5]–[8]. Traditonal semicondutor materials typically absorb all photons with energies larger than their band gap energies, and spectral selectivity in devices base on such materials is often achieved by adding exteral filters[9] or empirically controlling the thickness of the film, which adds complexity and cost to the system[10], [11]. In this work, we propose an alternate solution that aims to achieve controlled spectral selectivity within the absorbing film iteself: embedding photonic crystal (PC) structures in the absorbing film and tailoring the geometry of the PC structures to engineer the photonic band structure for sepectral selectivity.

PCs are materials with dielectric functions that vary periodically in one or more dimensons, potentially creating a photonic band gap that forbids photons within a range of frequencies to propogate within the material. Because of this

compelling mechanism, PCs have been well studied to manipulate light flow and successfully employed in many applications including optical communications[12]–[14] and optoelectronics[15]–[17].

Although photonic band structures can be easily tnuned in frequency by adjusting the length scale of the periodicity of the dielectric constant (lattice constant), PCs have been mostly engineered to have their phonic band gap lying in the lossless spectral range of the media, i.e. below the electronic band gap of the semiconductor where it can be treated like a simple dielectric material. Positioning the photonic band gap and bands of interest in the absorbing frequency range of the media is viewed as resulting in undesired loss in most optical communication and computing applications; however, semiconductor absorption and photogeneration are critical in optoelectronic applications such as photovoltaics and photodetectors. Engineering the photonic bands to fall within the absorbing frequency range of the semiconductor represents a potential new mechanism for spectral tuning.

Previous study on forming PCs in lossy materials, such as PCs constructed using metal nanoparticles, show that the reflection peaks diminish with increasing absorption.[18] Initial work applying PCs within the absorbing layer of solar cell has been reported, aiming to enhance absorption via spectrally selective light trapping and modulation of the density of states[19]-[21]. Rather than focusing on reflection or absorption alone, we present a comprehensive study of how embedding PCs within the absorbing media allow one to control the spectral features across multiple wavelength bands in absorption, reflectivity and transmittivity simultaneously, a promising route for complicated optoelectronic applications such as tandem solar cells. The concept is illustrated in Fig. 1. The normally incident light is expected to couple with in-plane photonic bands at the  $\gamma$  point of the Brillouin Zone and influence the out-of-plane reflection and transmission spectra.

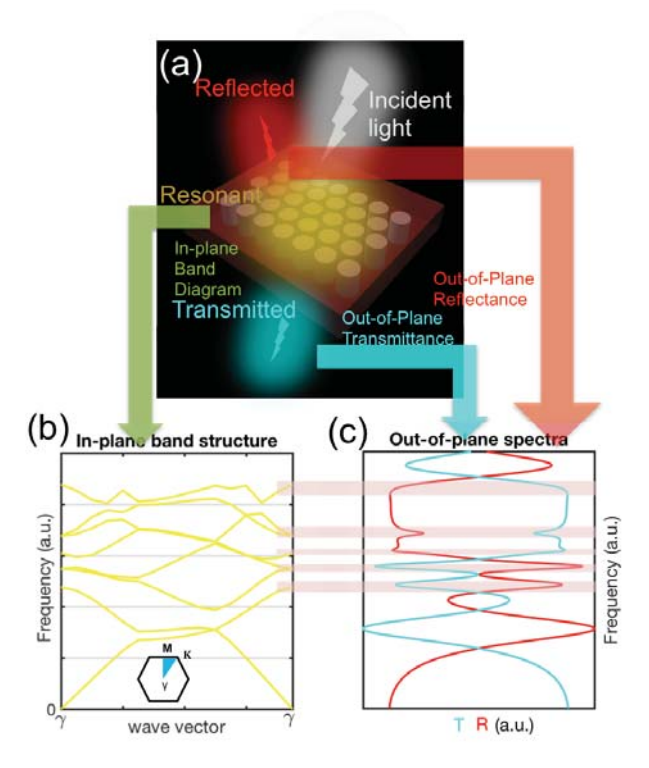


Fig 1. Schematic of a generic 2D slab PC structure illustrating the concept of PC-induced spectral selectivity. Broadband light (white color) is normally incident on the slab, with specific frequencies coupled to the resonance modes of the slab (yellow), tuning the spectral features in the out-of-plane transmission (blue) and reflection (red) profiles for spectral selectivity. A hypothetical photonic band diagram for the PC structure in (b) where the yellow lines are the bands and the inset shows where the  $\gamma$  point is in the Brillouin Zone. Hypothetical out-of-plane transmission and reflection spectra are also shown on the right as indicated by the arrows. The stripes connecting the two schematics illustrate the coupling between normal incidence light and in-plane-modes at the  $\gamma$  point of the Brillouin Zone.

In this study, we use finite-difference time-domain (FDTD) simulations and Fourier modal methods to quantify how absorption of the media affects the relevant in-plane bands that fall above the electronic band gap, as well as the out-of-plane transmission and reflection spectra. Experimentally we demonstrate a PC embedded in a semiconductor thin film structure: a self-assembled hexagonal polystyrene bead array infiltrated with PbS colloidal quantum dots (CQDs), which shows enhanced visible transparency over the non-structured film. This PC composite film shows promise for filterless visible-blind infrared photodetectors and top infrared cells in tandem solar cells.

### II. OPTICAL SIMULATIONS

To quantify the effect of material absorption on photonic band structure, we chose the well-studied PC structure composed of a 2D triangular lattice of air pillars in a GaAs slab with finite thickness. In FDTD simulations, we could artificially assign different aboseption strengths to the slab material by inputting different imaginary parts of the dielectric constant ( $\varepsilon_i$ ) while keeping the real part ( $\varepsilon_r$ ) constant, which is equivalent to varying the refractive index (n, k). Because of the requirement of satisfying the Kramers-Kronig relations [22], disperson is not considered in this test-case. The control dielectric case sets the  $\varepsilon_r$  as 13 to approximate the average value

for GaAs across the frequency range of interest and sets  $\epsilon_I$  to zero. We gradually increased  $\epsilon_i$  while keeping  $\epsilon_r$  at 13 in our simulations to quantify how dissipation affects photonic band structure.

We use the FDTD simulation method to calculate the photonic band structures [23]: our simulation volume includes an integer number of unit cells in the 2D plane, and the volume extends in the z-direction symetrically above and below the slab by approximately 10 lattice constants. For the x and y (in-plane) axes, we use Bloch boundary condtions, while for the z-axis, perfectly matched layers (PMLs) were applied with symetric or anti-symetric boundary condtions to distinguish the even (TE-like) and odd (TM-like) mode polarizations, respectively.

In order to position the photonic band gap above the electronic band gap of GaAs, we chose an air hole array with radius r = 60 nm and lattice constant a = 250 nm. The model structure is shown in the inset of Fig. 2(d). The simulated band structures are summarized in Fig. 2(a) with the dielectric case ( $\varepsilon_{\rm I} = 0$ ) in the top-left panel followed by a series of increasing  $\varepsilon_{\rm i}$  cases. The full GaAs calculation including dispersion is shown in Fig. 2(b).

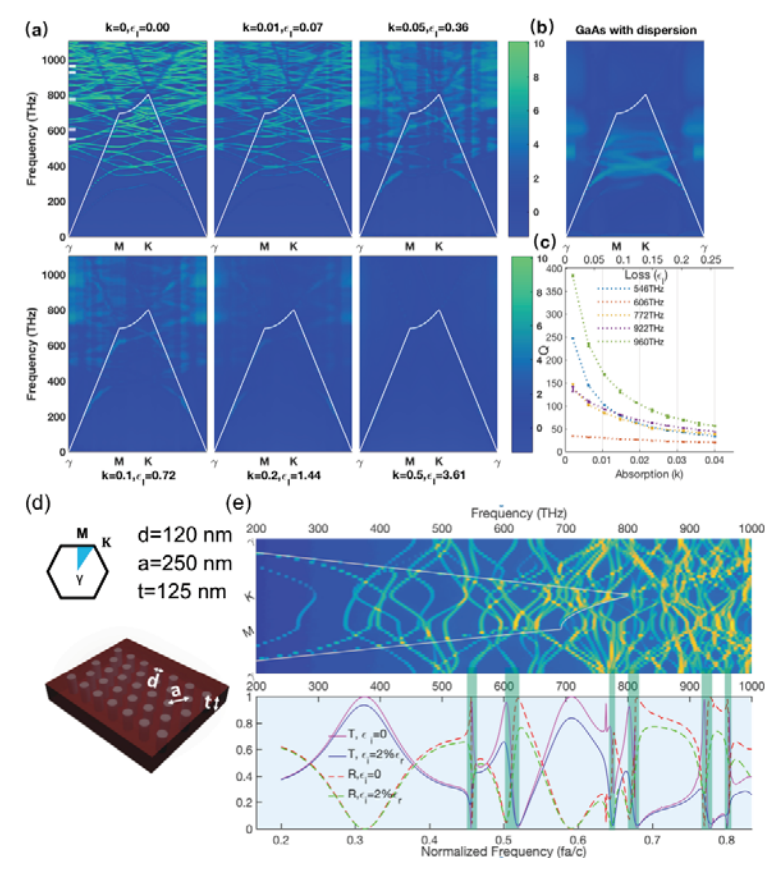


Fig 2. (a) Simulated photonic band diagrams using FDTD methods for the structure shown in the inset of (c). The  $\varepsilon_r$  is kept constant at 13 while the  $\varepsilon_i$  is varied from 0 to 3.61 from the top left panel to the bottom right panel in (a). The light lines are plotted in white, and the color scale is in arbitrary logarithmic units corresponding to field intensity. (b) Calculation for GaAs including dispersion. (c) Quality factor for the 5 selected modes with

frequency labeled by the white marks at the  $\gamma$  point in the top left panel of (a), as a function of increasing absorption (k) of the media. (d) Schematic of Brillouin Zone of the quasi-2D simulated PC structure: a triangular lattice of air pillars with diameter 120 nm, depth 125 nm, lattice constant 250 nm, and slab thickness 125 nm. (e) Bottom panel: out-of-plane transmission (solid lines) and reflection (dashed lines) spectra for normally incident fields calculated using FMM. The PC structure consists of a triangular lattice (lattice constant noted as a) of air pillars (radius notes as r) in a semiconductor slab (thickness noted as t) with r=0.24a, t=0.5a and  $\epsilon=13$  (non-absorbing case, pink and dashed red lines) and  $\epsilon=13+0.3i$  (absorbing case, blue and dashed green lines). Top panel: the corresponding photonic band structure for the non-absorbing case with the light line plotted in white. The resonance features of the out-of-plane spectra are highlighted and aligned with the associated modes at the  $\gamma$  point.

The results displayed in Fig. 2(a) show that the center frequenies of the bands remain almost unchanged while the widths of the bands broaden as the absorption strength increases. The clarity of the higher frequency bands decreases faster than that of the lower frequency bands, which is expected since the higher fequency bands experience higher rates of dissipation and have shorter absorption lengths. The rough maintenance of the photonic bands in the presence of weak material loss can be understood from perturbation theory applied to the PC master equation[17]. When a small imaginary part is added to the dielectric function  $\varepsilon$ , there will be an imaginary part added to the resonance frequency,  $\omega_0 = \omega_0 - i\gamma$ , which consequently adds to the linewidth of the Lorentzian resonance profile and reduces the resonance peak height.

In addition to showing the evolution of the band diagrams, we performed a quantitative study of the effect of dissipation on photonic band structures by calculating the quality factor (Q) for selected frequency bands. In this calculation, we chose five modes capable of coupling to normal incidence plane waves, which means they can be excited by incident plane waves and radiate energy to transmitted and reflected waves, giving them finite Q even without the presence of dissipation. From Fig. Q(C), we can see that the quality factors similarly decrease dramatically with presence of absorption, and the differences between the modes get smaller, causing a "smearing" and overlapping of the photonic bands until the bands eventually disappear at the limit of very high dissipation.

To understand how the in-plane photonic band structure interacts with incident waves and the effect of absorption on the out-of-plane spectra, we calculate the transmission and reflection spectra for absorbing and non-absorbing PC slabs via Fourier modal methods (FMM) [24]–[26] at a fixed in-plane wave vector with polarization along one of the reciprocal lattice vectors. The calculation results are shown in Fig. 2 (e).

The spectra consist of sharp Fano resonances features [27] over a smoothly varying background. The background spectrum arises from a simple Fabry-Perot cavity consisting of the thin-film and two film-air interfaces. The sharp resonances occur at the same frequencies as the in-plane radiating modes, which is expected because the transmitted and reflected fields directly couple to the incident field while simultaneously indirectly coupling to the radiating modes of the PC excited by the incident field. These resonances can be well explained by temporal-coupled wave theory [27]–[29]. We note that not all

modes in the bands can be excited by incident plane waves due to symmetry and polarization restrictions [27].

In the lossless case, the Fano resonance features are sharp and narrow due to the long lifetimes of the radiating modes that are essentially lossless. When there is dissipation, the lifetime of the radiating modes decreases, generating broader and weaker resonances, whose origin is the same as that of the quality factor reduction seen for the modes in the photonic band structures. The resonance frequencies remain almost unchanged with a  $\varepsilon_I$  value of 2% of  $\varepsilon_r$  which agrees with the FDTD photonic band structure simulations. The amplitude of the smoothly varying background is reduced, which is expected when the film becomes lossy.

The results suggest that one can use 2D PCs to enable fine spectral tuning in transmission, reflection and absorption. The broadband tramission and reflection spectra are primarily determined by the average optical properties of the film, i.e. the effective refractive index, which mainly depends on the volume ratio of the low index inclusions and properties of the materials. To target narrow band spectral selectivity, one can carefully design PC structures, whose tuning knobs include the periods, volume ratios, and refractive indices of the materials, to engineer the in-plane photonic bands to tune the out-of-plane spectra through the strong coupling between them.

# III. EXPERIMENTAL DEMONSTRATION

To experimentally demonstrate that 2D PC structures can be used to tune out-of-plane spectral selectivity, we fabricated a proof-of-principle PC structure in a strongly absorbing material with infrared responsivity. We chose a PbS CQD thin film as the media for its well-known infrared absorption, facile solution processability, and success in many optoelectronic applications, including light emitting diodes [30], photodetectors [31] and solar cells [32], [33]. We chose polystyrene beads to serve as the low index inclusions in the thin film, and we constructed a 2D monolayer triangular lattice structure via nanosphere self-assembly [34], [35].

We optimized the PC structure using FDTD simulations for a high visible transparency infrared abosrbing film application. The simulated spectra are shown in Fig. 3(a). To mimic a realistic system with large-scale non-uniformity, based on our experimental thickness measurements, the transmission was calculated by averaging 11 different film thicknesses for the PC-CQD case  $(250 \pm 50 \text{ nm})$  and 3 differenet film thicknesses for the CQD control case (200  $\pm$  10 nm). The fabrication strated with treating glass substrates with O2 plasma for hydrophilicity. We spin-cast 50 µL of a 10% w/v aqueous polystyrene bead solution (Magsphere) at 500 rpm for 10 seconds followed by a 2-minute 700 rpm drying step. The beads self-assemble to form a triangular lattice monolayer array with a lattice constant equal to the bead diameter. O<sub>2</sub> plasma at 120 W for a few minutes was then used to etch the beads to open up space between the beads to tune the radius-tolattice-constant ratio. A scanning electron microscope (SEM) image of the bead array after etching is shown in the inset of Fig. 3(b), and the inset of the SEM image is a photograph of a 1 inch x 1 inch sample with strong irridescence from the beads, indicating large-scale oder. Our oleic-acid capped PbS CQD

solution was synthesized using previouly published methods [36]. Starting with 50 mg/mL solution of PbS CQDs in octane, a solid state 3-mercaptopropionic acid (MPA) ligand exhange layer-by-layer process was used to build the CQD film. To promote the infiltration of CQDs into the open space of the bead array structure, the bead arrays were treated with 5% MPA in methanol via spin-casting at 1000 rpm spining for 10 seconds before spin-casting the CQD solution at 2500 rpm. The insets of Fig.3 (b) are the PC structures before and after CQD infiltration, showing that the beads array is preserved after infiltration.

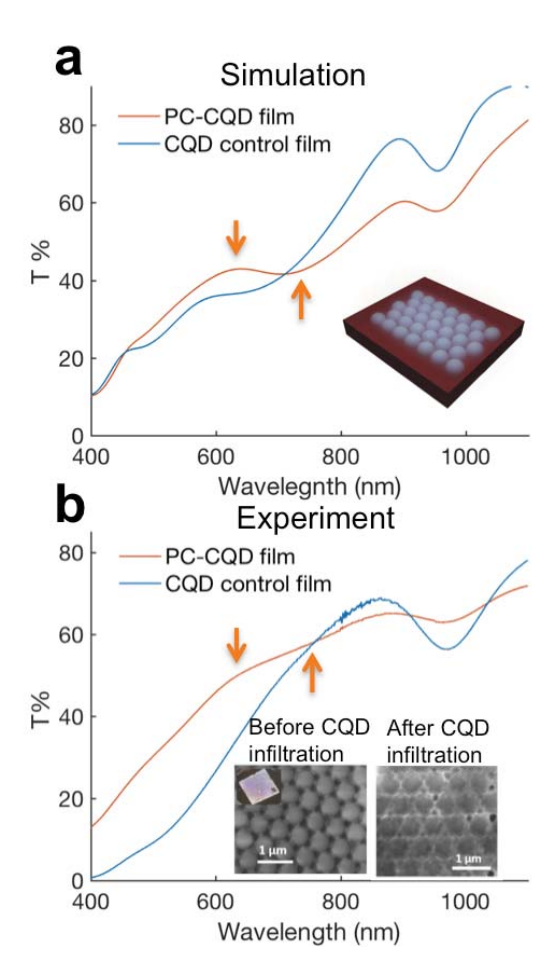


Fig. 3. (a) FDTD simulated transmission spectra for a PC-CQD film and a control CQD film, with PC-CQD film showing slightly enhanced visible transparency. The inset is a rendering of the simulated PC-CQD structure: a monolayer triangular lattice of polystyrene beads infiltrated with PbS CQDs. The control film has an average thickness of 200 nm, and the PC-CQD film averages 250 nm thick. It has a lattice constant of 250 nm. (b) Experimentally measured transmittance spectra using UV-Vis-NIR spectrophotometery, qualitatively matching the simulation results. The difference in magnitude of the transmittance is probably due to the large-area non-uniformities and roughness of the experimental film. Insets are top-view SEM images of the bead array before and after CQD infiltration.

The transmittance spectra were measured by placing the sample at the entrance of an integrating sphere and focusing light onto the sample using a transmittance lens and a UV-Vis-

NIR spectrophotometer. The experimental spectra qualitatively match the simualted spectra, both showing enhanced visible transparency over the control case with a peak in the visible range of the PC-CQD spectrum near 630 nm. The presence of surface roughness and non-uniformity across the film is expected to reduce the interference effects, broadening and reducing the intensity of the peaks and valleys in the experimental spectra. Although preliminary, these results show the promise of using PC structures in absorbing media as tuning knobs for spectral selectivity in optoelectronic applications.

# IV. SUMMARY AND OUTLOOK

We proposed and analyzed a new strategy to tune the outof-plane spectral selectivity of optoelectronic thin films by engineering in-plane photonic band structures within the abosorbing frequency range of semiconductors. Quantitative analysis of the impact of absorption on the photonic band structure was performed and the effect of absorption on the out-of-plane spectra was studied. Combining photonic band structure simulations with FMM analysis, our results show that coupling between the in-plane photonic bands at the  $\gamma$  point and normal incidence light will induce sharp Fano resonance features on top of the smoothly varying background reflection and transmission spectra, even in the presence of material absorption. These results show that adjusting the parameters of a PC structure embedded in an absorbing material could produce spectrally selective optoelectronic films for targeted applications. Experimentally, we also demonstrated a proof-ofprinciple self-assembled PC structure consisting of a polysterene bead array in a PbS CQD matrix that produced enhanced visible transparency over a control CQD-only film, showing promise for multijunction and transparent photovoltaics.

Because of the flexibility and ease of fabrication of solution-processed materials, future work will focus on introducing dispersion into the optical models of these materials and designing PC structures in realistic solution-processed optoelectronic films to optimize their spectral selectivity for specific applications such as narrow-band infrared photodetectors and multijunction solar cells.

### ACKNOWLEDGMENTS

The authors would like to thank A. Rauch, E. Tsai, and M. Wagenmaker for useful disscussion and assistance with preliminary calculations for this work.

#### REFERENCES

- [1] D. Bračun, G. Škulj, and M. Kadiš, "Spectral selective and difference imaging laser triangulation measurement system for on line measurement of large hot workpieces in precision open die forging," *Int J Adv Manuf Technol*, vol. 90, no. 1–4, pp. 917–926, Apr. 2017.
- [2] J. J. Talghader, A. S. Gawarikar, and R. P. Shea, "Spectral selectivity in infrared thermal detection," *Light: Science & Applications*, vol. 1, no. 8, p. e24, Aug. 2012.
- [3] J. A. Ratches, R. H. Vollmerhausen, and R. G. Driggers, "Target acquisition performance modeling of infrared imaging systems: past,

- present, and future," *IEEE Sensors Journal*, vol. 1, no. 1, pp. 31–40, Jun. 2001.
- [4] C. S. Goldenstein, R. M. Spearrin, J. B. Jeffries, and R. K. Hanson, "Infrared laser-absorption sensing for combustion gases," *Progress in Energy and Combustion Science*, vol. 60, pp. 132–176, May 2017.
- [5] A. D. Vos, "Detailed balance limit of the efficiency of tandem solar cells," J. Phys. D: Appl. Phys., vol. 13, no. 5, p. 839, 1980.
- [6] E. H. Sargent, "Infrared photovoltaics made by solution processing,"
   *Nature Photonics*, vol. 3, no. 6, pp. 325–331, Jun. 2009.
   [7] D. M. Trotter and A. J. Sievers, "Spectral selectivity of high-
- [7] D. M. Trotter and A. J. Sievers, "Spectral selectivity of hightemperature solar absorbers," *Appl. Opt., AO*, vol. 19, no. 5, pp. 711– 728, Mar. 1980.
- [8] H. Kim, H.-S. Kim, J. Ha, N.-G. Park, and S. Yoo, "Empowering Semi-Transparent Solar Cells with Thermal-Mirror Functionality," Advanced Energy Materials, vol. 6, no. 14, p. 1502466, Jul. 2016.
- [9] H. Hara, N. Kishi, M. Noro, H. Iwaoka, and K. Suzuki, "Fabry-Perot filter, wavelength-selective infrared detector and infrared gas analyzer using the filter and detector," US6590710B2, 08-Jul-2003.
- [10] K. A. Bush et al., "23.6%-efficient monolithic perovskite/silicon tandem solar cells with improved stability," *Nature Energy*, vol. 2, no. 4, p. 17009, Apr. 2017.
- [11] X. Wang et al., "Tandem colloidal quantum dot solar cells employing a graded recombination layer," *Nature Photonics*, vol. 5, no. 8, pp. 480–484, Aug. 2011.
- [12] J. C. Knight, T. A. Birks, P. S. J. Russell, and D. M. Atkin, "All-silica single-mode optical fiber with photonic crystal cladding," *Opt. Lett.*, *OL*, vol. 21, no. 19, pp. 1547–1549, Oct. 1996.
- [13] E. Kuramochi et al., "Large-scale integration of wavelength-addressable all-optical memories on a photonic crystal chip," Nature Photonics, vol. 8, no. 6, pp. 474–481, Jun. 2014.
- [14] M. Notomi et al., "Low-power nanophotonic devices based on photonic crystals towards dense photonic network on chip," IET Circuits, Devices & amp; Systems, vol. 5, no. 2, pp. 84–93, Mar. 2011.
- [15] H.-G. Park et al., "Electrically Driven Single-Cell Photonic Crystal Laser," Science, vol. 305, no. 5689, pp. 1444–1447, Sep. 2004.
- [16] P. Bermel, C. Luo, L. Zeng, L. C. Kimerling, and J. D. Joannopoulos, "Improving thin-film crystalline silicon solar cell efficiencies with photonic crystals," *Opt. Express, OE*, vol. 15, no. 25, pp. 16986– 17000, Dec. 2007.
- [17] J. D. Joannopoulos, S. G. Johnson, J. N. Winn, and R. D. Meade, Photonic Crystals: Molding the Flow of Light - Second Edition. Princeton University Press. 2011.
- [18] Z. Wang, C. T. Chan, W. Zhang, N. Ming, and P. Sheng, "Three-dimensional self-assembly of metal nanoparticles: Possible photonic crystal with a complete gap below the plasma frequency," *Phys. Rev. B*, vol. 64, no. 11, p. 113108, Aug. 2001.
- [19] K. Xingze Wang, Z. Yu, V. Liu, A. Raman, Y. Cui, and S. Fan, "Light trapping in photonic crystals," *Energy & Environmental Science*, vol. 7, no. 8, pp. 2725–2738, 2014.

- [20] J. R. Tumbleston, D.-H. Ko, E. T. Samulski, and R. Lopez, "Absorption and quasiguided mode analysis of organic solar cells with photonic crystal photoactive layers," *Opt. Express, OE*, vol. 17, no. 9, pp. 7670–7681, Apr. 2009.
- [21] A. Chutinan and S. John, "Light trapping and absorption optimization in certain thin-film photonic crystal architectures," *Phys. Rev. A*, vol. 78, no. 2, p. 023825, Aug. 2008.
- [22] V. Lucarini, J. J. Saarinen, K.-E. Peiponen, and E. M. Vartiainen, Kramers-Kronig Relations in Optical Materials Research. Springer Science & Business Media, 2005.
- [23] I. A. Sukhoivanov and I. V. Guryev, *Photonic Crystals: Physics and Practical Modeling*. Berlin Heidelberg: Springer-Verlag, 2009.
- [24] L. Li, "New formulation of the Fourier modal method for crossed surface-relief gratings," *Journal of the Optical Society of America A*, vol. 14, no. 10, p. 2758, Oct. 1997.
- [25] L. Li, "Formulation and comparison of two recursive matrix algorithms for modeling layered diffraction gratings," *Journal of the Optical Society of America A*, vol. 13, no. 5, p. 1024, May 1996.
- [26] L. Li, "Use of Fourier series in the analysis of discontinuous periodic structures," *Journal of the Optical Society of America A*, vol. 13, no. 9, p. 1870, Sep. 1996.
- [27] Haus H. A., Waves And Fields In Optoelectronics. N.J.: Prentice Hall, Englewood Cliffs, 1984.
- [28] Wonjoo Suh, Zheng Wang, and Shanhui Fan, "Temporal coupled-mode theory and the presence of non-orthogonal modes in lossless multimode cavities," *IEEE Journal of Quantum Electronics*, vol. 40, no. 10, pp. 1511–1518, Oct. 2004.
- [29] S. Fan, W. Suh, and J. D. Joannopoulos, "Temporal coupled-mode theory for the Fano resonance in optical resonators," *Journal of the Optical Society of America A*, vol. 20, no. 3, p. 569, Mar. 2003.
- [30] X. Gong et al., "Highly efficient quantum dot near-infrared lightemitting diodes," Nature Photonics, vol. 10, no. 4, pp. 253–257, Apr. 2016.
- [31] G. Konstantatos et al., "Ultrasensitive solution-cast quantum dot photodetectors," *Nature*, vol. 442, no. 7099, pp. 180–183, Jul. 2006.
- [32] G. H. Carey, A. L. Abdelhady, Z. Ning, S. M. Thon, O. M. Bakr, and E. H. Sargent, "Colloidal Quantum Dot Solar Cells," *Chem. Rev.*, vol. 115, no. 23, pp. 12732–12763, Dec. 2015.
- [33] E. S. Arinze et al., "Color-tuned and transparent colloidal quantum dot solar cells via optimized multilayer interference," Opt. Express, OE, vol. 25, no. 4, pp. A101–A112, Feb. 2017.
- [34] M. M. Adachi, A. J. Labelle, S. M. Thon, X. Lan, S. Hoogland, and E. H. Sargent, "Broadband solar absorption enhancement via periodic nanostructuring of electrodes," *Scientific Reports*, vol. 3, p. 2928, Oct. 2013
- [35] C. L. Cheung, R. J. Nikolić, C. E. Reinhardt, and T. F. Wang, "Fabrication of nanopillars by nanosphere lithography," *Nanotechnology*, vol. 17, no. 5, p. 1339, 2006.
- [36] A. H. Ip et al., "Hybrid passivated colloidal quantum dot solids," Nature Nanotechnology, vol. 7, no. 9, pp. 577–582, Sep. 2012.